Effect of Seepage Barrier in Steady Seepage Below Earthen Dam by Centrifuge Modeling

Smita Tung, Sibapriya Mukherjee, and Gupinath Bhandari

1 Introduction

The effect of seepage water flow causes loss of inter-particle force leading to a decrease in the skeleton stress which triggers dam failures as well as induced slope instability. According to the studies, approximately 41.6% of dam failures are related to internal erosion [1]. A comprehensive discussion on the mechanisms of piping and internal erosion in dams was presented by McCook [2]. Fell and Wan [3] presented methods for estimating the probability of failure of embankment dams by internal erosion, piping within the foundation, and piping from the embankment to the foundation. Cut-off walls are used to prevent seepage in dams as a long-term effective solution.

Approaches of centrifuge modeling have facilitated the evaluation of seepage and deformation in the embankments and are also considered a powerful tool to examine the failure mechanisms. Centrifuge modeling generates the real stress field and at the same time faster seepage flow. Centrifuge modeling is a technique that involves physical modeling to capture the correct failure mechanism in the boundary value problems with the help of digital cameras.

The basic principle of a geotechnical centrifuge is to enhance the gravity field by the same geometric factor N, relative to the normal earth's gravity field. In a

S. Tung (✉)
Assistant Professor, Department of Civil Engineering, GLA University, Mathura 281406, India

S. Mukherjee
Professor, Department of Civil Engineering, Jadavpur University, Kolkata 700092, India
e-mail: sibapriya.mukherjee@jadavpuruniversity.in

G. Bhandari
Associate Professor, Department of Civil Engineering, Jadavpur University, Kolkata 700092, India
e-mail: gupinath.bhandari@jadavpuruniversity.in

C. N. V. Satyanarayana Reddy et al. (eds.), *Dynamics of Soil and Modelling of Geotechnical Problems*, Lecture Notes in Civil Engineering 186,
https://doi.org/10.1007/978-981-16-5605-7_17

centrifuge, small-scale models are tested in a gravity field, which is a linear function of the distance from the center of rotation. Thus, the gravity field varies linearly with radius from the center of rotation and as a square of the angular velocity $\dot{\theta}$ of the centrifuge.

A seepage study was carried out for the western dyke of Wallace dam (Lake Oconee, Georgia, USA) by Aral and Maslia [4]. It was observed that the flow vector to the chimney drain showed that it was very effective in reducing seepage pressures.

Davies and Parry [5] conducted a centrifuge test to check the performance of low embankment founded on soft clay soil during and after the construction. They monitored displacement and pore pressure variation to observe the progressive failure. They carried out total and effective stress analyses of the embankment stability. The pore pressure studied increased as much as 18% after the end of the construction. Perri et al. [6] analyzed the influence of the pore water pressures in the calculated factor of safety of an embankment with and without cut-off wall in steady-state condition of full flooding stage using finite element method. They observed that using cut-off wall there was a significant decrease in seepage gradient and thereby an increase of Factor of Safety.

The present study has taken up a field problem in the Sunderbans region of West Bengal, India, where 3520 km of earthen embankments, used as protective structures of water heads of 3–4.5 m. The Sunderbans along the Bay of Bengal has evolved through quaternary sediments deposited mainly carried by the complex network of tidal rivers. It is part of the tide-dominated lower deltaic plain.

The purpose of this study is to find the effect of cut-off wall beneath an earthen dam for analyzing the failure by the use of centrifuge modeling as a tool. Experimental testing procedures were implemented as part of a recent centrifuge study undertaken to evaluate the performance of slopes at failure. In the experimental simulation, phreatic line, flow net, and stability against steady-state seepage in terms of factor of safety have been obtained. The effectiveness of sheet pile as seepage barrier, varying sheet pile length and position for all cases, have been studied, with the variation of sheet pile length of 5 m, 10 m, 15 m, and 20 m varying the sheet pile position at $B/8$, $2B/8$, and $3B/8$ positions from the downstream end, B being the width of the dam. It has been observed that sheet pile length has a significant effect on pore pressure variation along the sheet pile. It also evaluated by experimental modeling that seepage failure is more likely to occur at the bottom of cut-off walls because of the magnitude of high seepage velocity. The average seepage gradient of the embankment foundation decreases with the increase of the height of cut-off walls, and the seepage gradient at the bottom of cut-off walls is always maximum along the seepage contour line.

2 Model for the Study

The stratification of the subsoil of the selected area of South 24 Parganas, West Bengal, has been obtained from the study of bore log data sheets of different locations.

The cross-sectional details of the existing embankment of the typical model dam have been presented in Fig. 1. The study has been done for working head of 3.0 m in steady-state condition. Table 1 presents sheet pile properties for steady seepage and transient condition.

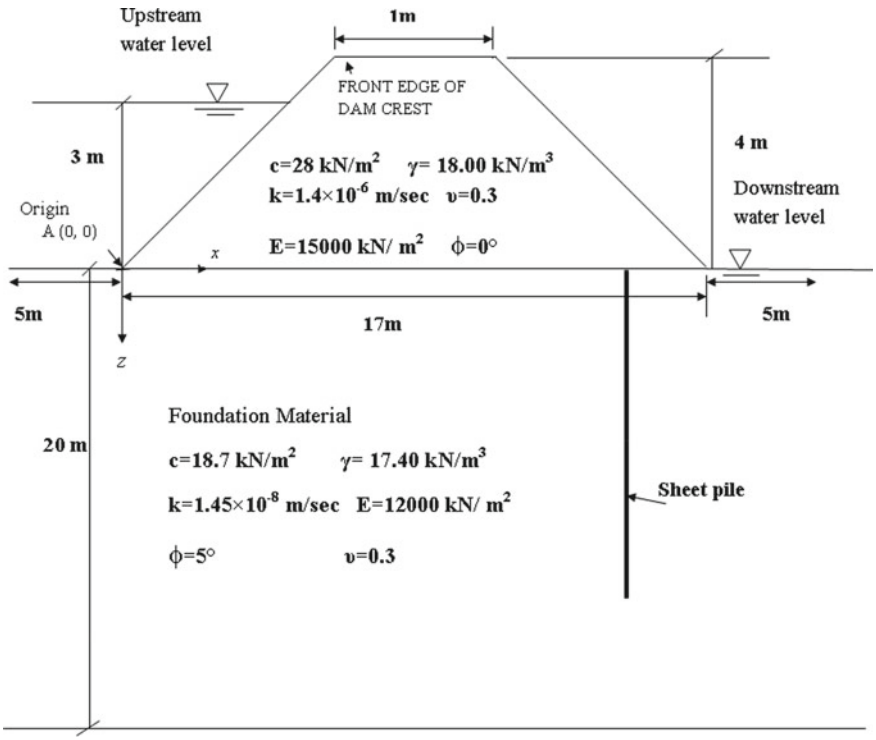

Fig. 1 Schematic diagram of the model embankment for centrifuge modeling

Table 1 Properties of sheet pile material

Area of cross-section per meter	0.03
Moment of Inertia per meter (N-m/m)	0.00225
E_{steel} (N/m^2)	2×10^{11}

3 Centrifuge Modeling

3.1 Description of Centrifuge

This geotechnical centrifuge at the Geotechnical Engineering Laboratory, Civil Engineering Department, Jadavpur, is a 4 pole 500 Hz induction motor with 3 phase system and of a 1.5 m radius with a maximum payload capacity of 8.5 tons at 400 g. The diameter of the centrifuge is 0.55 m. The turner beam carries a scaled model at one end and a counterweight at the other, each mounted on a swing platform has been described in Fig. 2. In the geotechnical centrifuge considering 100 g the calculated rpm is 404 rpm using Eq. (1).

$$\omega^2 R = ng \tag{1}$$

$$\omega = \sqrt{\frac{100 \times 9.81}{0.55}} = 42.23 \text{ rad/s} = 404 \text{ rpm} = 400 \text{ rpm (say)}$$

In centrifuge modeling, a rotating soil body is mounted on a geotechnical centrifuge to represent a scale model of a given prototype that is to be modeled.

The ratio of linear prototype dimension to the centrifuge model when N, then the ratio of area is N^2 and volume N^3. It has been indicated from the scaling relation that the forces in the prototype are N^2 times and moments N^3 of the corresponding model. In the experiment, it was necessary to design model wall to a similar stiffness of prototype per unit width (EI). The ratio of stiffness of the prototype is N^3 times that of the model. In the present study, N has been adopted as 100. The model was

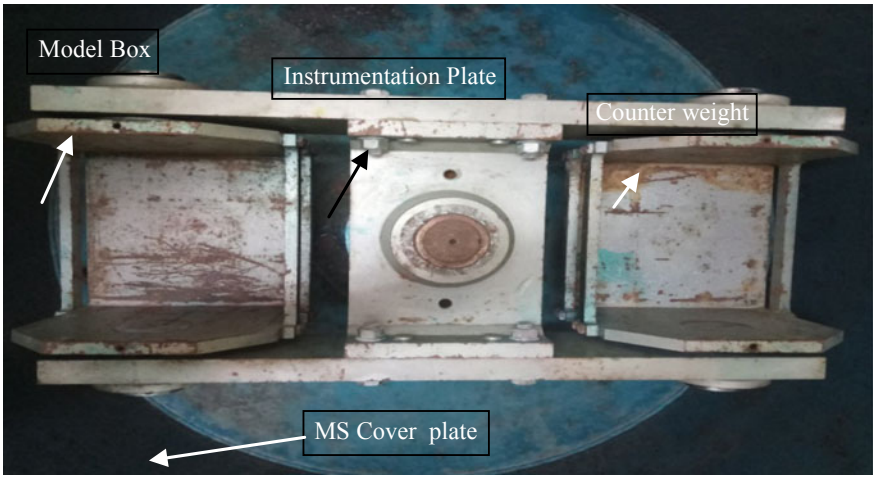

Fig. 2 Top view of the geotechnical centrifuge with component details

1/100 of the prototype linear dimension, and the model acceleration was 100 times of normal terrestrial gravity. In order to determine the true stiffness (EI) of the modeled sheet pile wall, $EI_{\text{model}} = EI_{\text{prototype}}/N^3$.

Steel sheet pile has been considered as prototype structure. Modulus of Elasticity of Steel Sheet pile ($E_{\text{prototype}}$) $= 2 \times 10^{11}$ N/m^2. Moment of Inertia per meter of steel sheet pile ($I_{\text{prototype}}$) $= 0.00225$ m^3. In the present seepage study, Perspex sheet has been used as modeled sheet pile. Modulus of Elasticity (E_{model}) of the Perspex $= 2.0 \times 10^9$ Pa. Moment of Inertia per unit width (I) of a rectangular cross-section is $\frac{(h')^3}{12}$, where h' is the section depth. In the present experimental study, 20 cm length of Perspex when modeled as sheet pile, Moment of Inertia per unit width (I_{model}) $= 2.49 \times 10^{-7}$ m^3/m.

$$EI_{\text{model}} = 2.0 \times 10^9 \times 2.49 \times 10^{-7} = 498 \text{ N-m/m}.$$

3.2 Experimental Setup

3.2.1 Test Box

The scaled model and the counterweight have been mounted at two ends of a swing platform. A seepage square tank has been fabricated with a steel frame, supporting a 10 mm thick transparent Perspex sheet on all sides to simulate three-dimensional conditions. The test box has dimensions of 26.7 cm (Length) by 26.7 cm (Width) by 26.7 cm (Height).

Water Supply Arrangement Using Valve

The reservoir has been placed above the top of the tank and the flow from reservoir to tank has been taken by virtue of centrifugal acceleration. In this study, Arduino ATMEGA 2560 board has been used to control the inlet and outlet valve. An artificial tide control circuit to provide an interface to complete the experimental work. The circuit has been processed by providing an internal energy source and has been controlled by an infrared remote.

Digital Image Processing

With the help of digital cameras, it has been possible to capture the digital image of the centrifuge model by mounting the camera on the model and viewing the cross-section through the transparent side. To fulfill the objective, Raspberry Pi 3B model has been used with a preinstalled Wi-Fi hardware module.

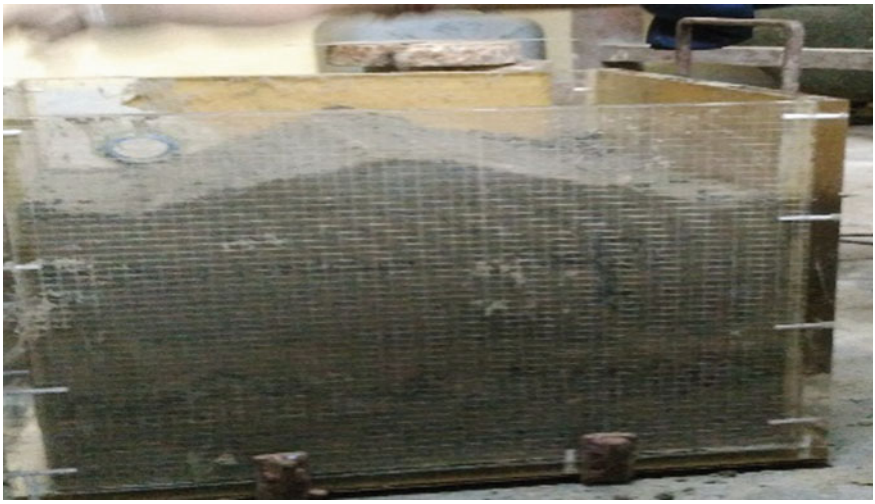

Fig. 3 Top view of the geotechnical centrifuge with component details

Construction of Model Embankment

Embankment model was formed as a typical earthen embankment with desired dimensions and properties and a centrifuge scale of $N = 100$ has been shown in Fig. 3.

A 20 cm thick bed was constructed in five layers was achieved by blows from a Standard Proctor Hammer of 4.5 kg falling over a height of 300 mm. The number of blows was adjusted as per the density requirement. The targeted density was 95% of Standard Proctor density. The Soil properties of the embankment as per IS classification is ML. The side slopes were kept at 2(H):1(V). Sheet piles were used as a cutoff in the experimental model in the centrifuge. Table 2 represents numerical analysis for the current study considering a variation of parameters of sheet pile length and positions under steady-state conditions.

4 Results and Discussion

During steady-state tests with a working head of 3.0 m, the flow net pattern has been shown in Fig. 4 for the embankment. The variation of the flow net in the upstream side with respect to the working head condition has also been shown in the respective figures. Points A, B, C, D, E have been marked with the progress of time to illustrate the propagation of flow.

Table 2 List of centrifuge modeling cases under steady state

Sl. no	Sheet pile length in meter	Sheet pile position from the downstream end
1	N.A	N.A
2	5	*B*/8
3	10	
4	15	
5	20	
6	5	2*B*/8
7	10	
8	15	
9	20	
10	5	3*B*/8
11	10	
12	15	
13	20	

Where B = Base width of dam. Based on the images obtained from the experiments, phreatic line and flow net has been obtained for each experimental model against steady-state seepage condition

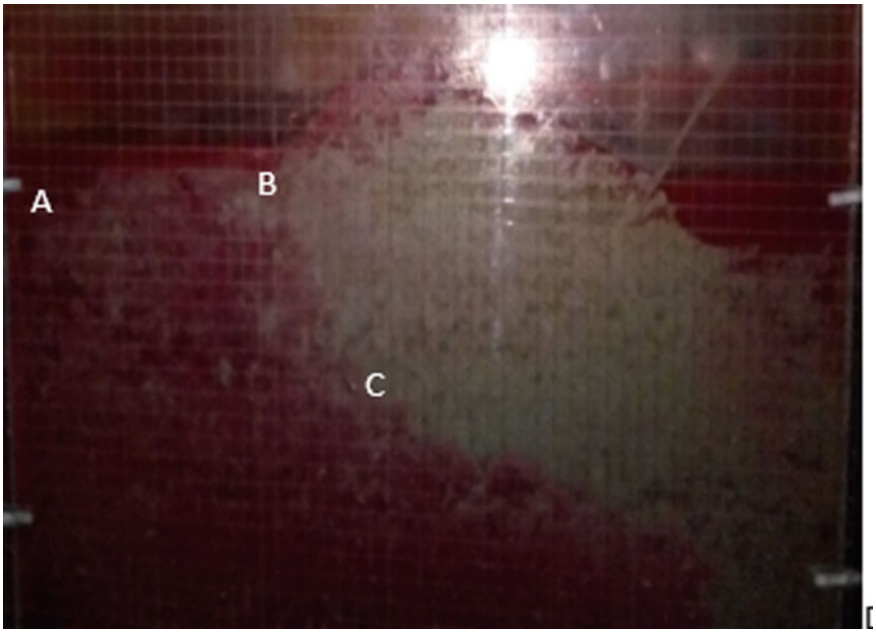

Fig. 4 Experimental output of embankment during steady-state condition without cutoff

4.1 Flow Net Pattern

An attempt has been made to observe the effect of location and length of sheet pile, used, as seepage cutoff. The results of the tests have been obtained by processing the captured image through MATLAB programming PIV High-resolution images that can be obtained from centrifuge model tests have been processed to give the fluid flow vector by Particle Image velocimetry (PIV) technique. PIV is a non-intrusive velocity field mapping technique that makes use of captured optical images to produce instantaneous vector measurements. Furthermore, PIV allows for the visualization of magnitudes and gives values the x–y components of velocity for the flow at different points, at different times in matrix form. The flow net has been developed for different cases under steady seepage conditions and also in different time intervals by image processing through PIV. The experimentally obtained phreatic surface, flow net, and pattern of fluid flow vector of an embankment has been shown in Fig. 5. The experimentally obtained typical phreatic surface, flow net, and pattern of fluid flow vector in an embankment for *B*/8 position 10 m length and 15 length sheet pile has been shown for in Fig. 7 and Fig. 8, respectively. A typical phreatic surface and flow net have been shown in Fig. 6 for the sheet pile at 3*B*/8 position 10 m length.

It has been observed from Figs. 6, 7, and 8 that that sheet pile acts as a fluid barrier effectively. It has been observed that as the Sheet pile moves away from the

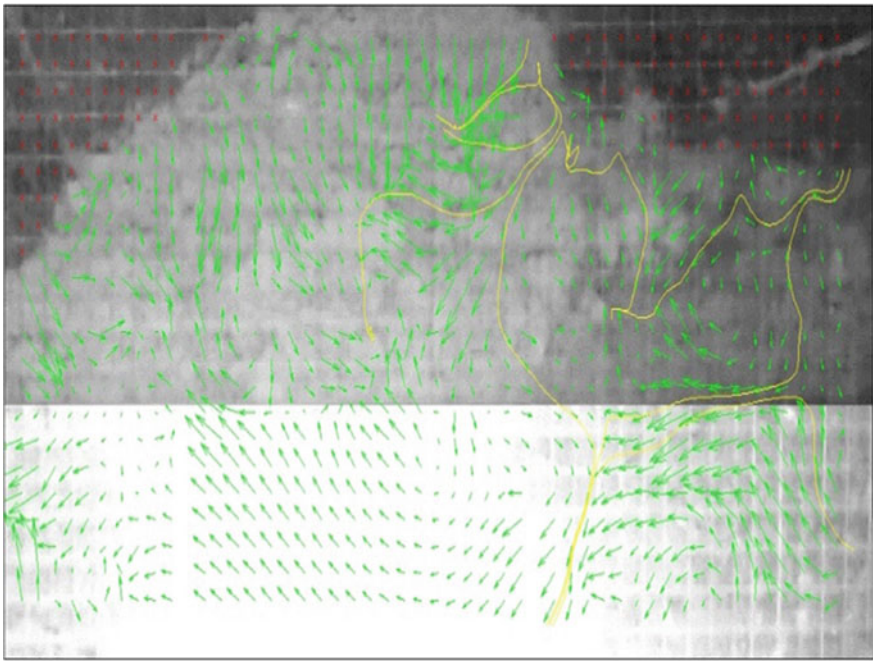

Fig. 5 Phreatic surface and flow net for steady-state condition

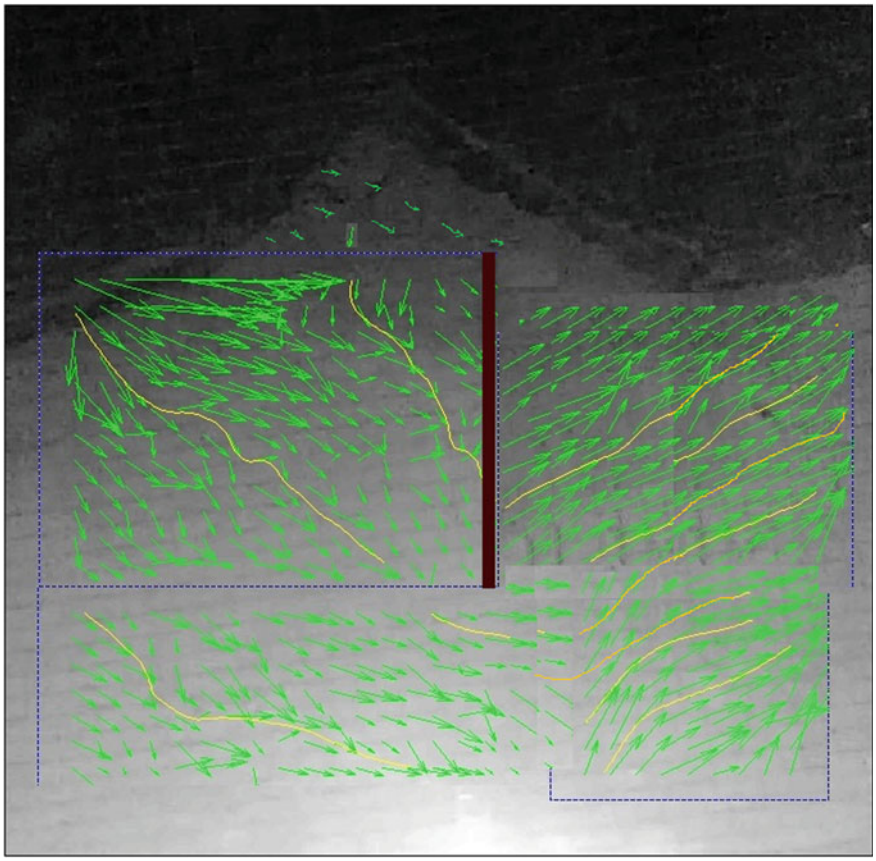

Fig. 6 Flow net and fluid flow vector for 3*B*/8 position 10 m long sheet pile

downstream end the field of the flow net near the downstream end is becoming more or more effective. When the sheet pile is shifted toward the downstream end, then the average dimension of the last element of the flow line is decreased. It also observed that for any fixed position when sheet pile length increases seepage path increases. It has been observed that for any fixed position of sheet pile exit gradient reduces with sheet pile length for any particular position of sheet pile. As sheet pile length increases seepage path increases which reduces the exit gradient. It has been observed when sheet pile length increases by 30% of the bottom width of the dam the exit gradient decreases to 9.97%. Furthermore, it evaluated that, If the sheet pile length increases 59% of bottom width of dam the exit gradient decreases by 18.16%. Therefore, from the modeling of seepage analysis, it is evaluated that if the sheet pile length increases 30–59% of the bottom width of the dam the exit gradient decreases of exit gradient is almost proportional to the pile length. From experimental modeling of seepage

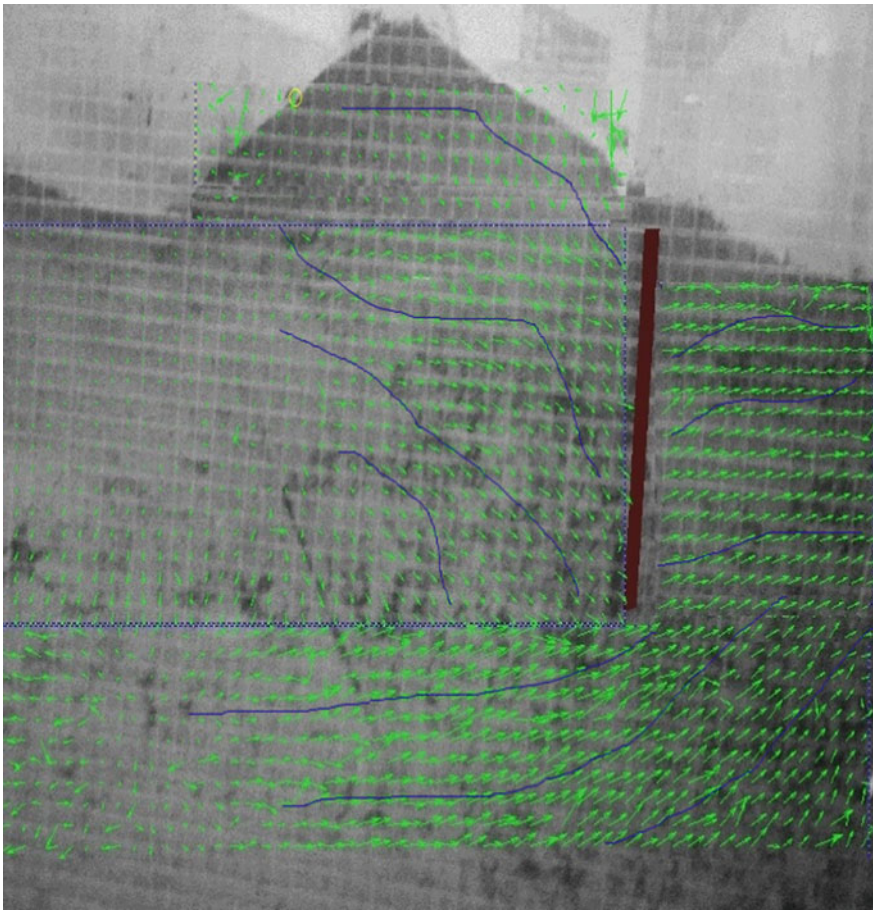

Fig. 7 Flow net and fluid flow vector for *B*/8 position 15m long sheet pile

analysis, it is evaluated that exit gradient decreases by 8.17% if the sheet pile position is shifted from 14.25% of the bottom width of the dam from the downstream end.

4.2 Fluid Flow Vector

An attempt has been made in this section to study the development of fluid flow vector with a variation of time without and with sheet pile depending on sheet pile lengths and positions. In each case, fluid flow vectors have been plotted along the horizontal profile at distances of 5 m from the top of the dam to study its variation within the dam body as well as the foundation of the dam. The purpose of this fluid flow vector study is to investigate the effectiveness of sheet piles against erosion

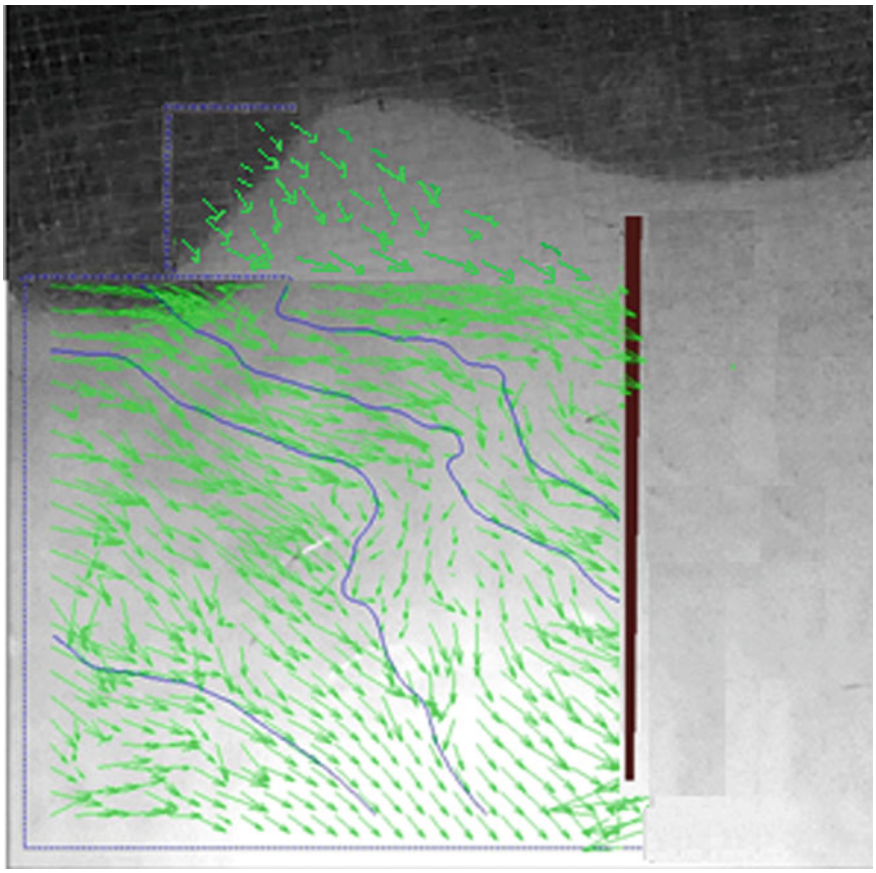

Fig. 8 Flow net and fluid flow vector *B*/8 position 10 m long sheet pile

caused by piping. Distance and velocity components in vertical direction have been plotted in the form of pixel/frame through PIV analysis.

Figure 9 represents a typical figure of fluid flow vector in pixel form analyzed by PIV for 10 m length of sheet pile positioned at *B*/8 position from downstream end along the horizontal direction. Figure 10 represents a typical figure of fluid flow vector analyzed by PIV for different length of sheet pile positioned at 3*B*/8 position from downstream end along the horizontal direction.

It is observed from Figs. 9 and 10 that maximum flow vector occurs at sheet pile position. This maximum value is highest for the 3*B*/8 position of sheet pile from the downstream end. For each case, the flow vector is increased at the sheet pile position indicating vertical flow along the sheet pile. The negative signs arise due to fluid flow in the downward direction along the length of the sheet pile. At the position of sheet pile, there is an abrupt jump of the fluid flow vector. At the upstream side of sheet pile, the fluid flow vector decreases along the length and at the downstream side of

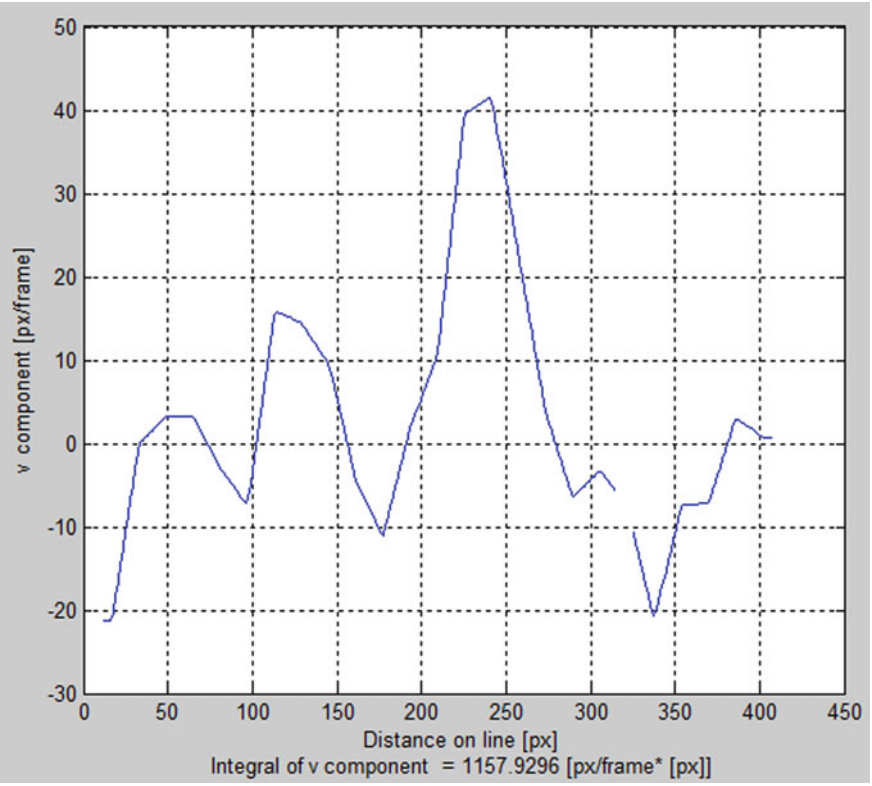

Fig. 9 Fluid flow vector in the vertical direction for sheet pile length 10 m at a fixed position of *B*/8

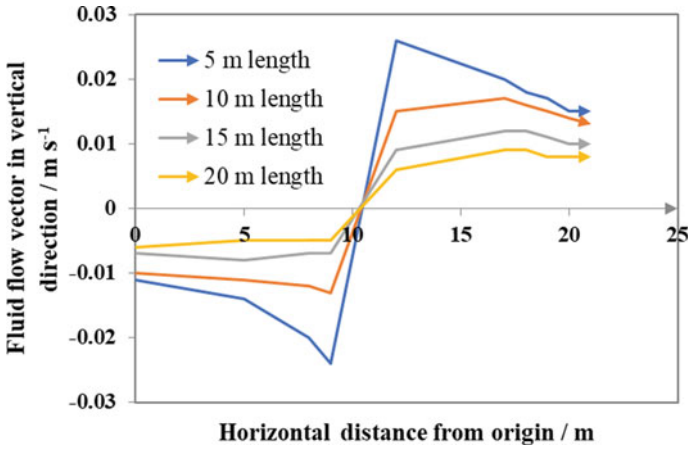

Fig. 10 Fluid flow vector in the vertical direction for different sheet pile lengths at a fixed position of 3*B*/8

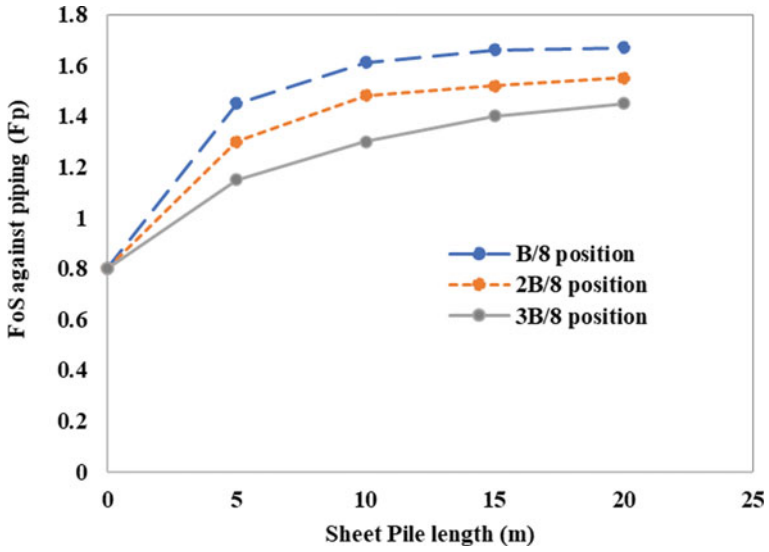

Fig. 11 Variation of the factor of safety with sheet pile position and length

sheet pile it increases with length. It has also been observed from Fig. 10 that the decrease of fluid flow vector for 20 m length of sheet pile on the downstream end is 30% less compared to 5 m length of sheet pile and 13% less compared to 15 m length of sheet pile at 3*B*/8 position. It has also been observed that the effect of sheet pile position on fluid flow vector on the downstream end is minimal.

4.3 Stability Against Piping

Figure 11 shows the variation of factor of safety against piping with sheet pile lengths at different positions.

It is observed that for a fixed sheet pile length, the factor of safety against piping decreases when the sheet pile position moves away from the downstream end. When sheet pile moves from downstream end, exit gradient increases and the chance of piping is reduced. As sheet pile position is shifted toward the downstream end, the average flow length of the extreme field of flow net at downstream end increases which causes a reduction in exit gradient. Thus, the factor of safety against piping increases. As sheet pile length increases seepage path increases, reducing the exit gradient and thus also reducing the chance of piping failure. A similar observation was made by Perri et al. [6]. For increase of the length of sheet pile, as creep length increases, exit gradient reduces and thereby factor of safety against piping increases. It has been seen that at 5 m of sheet pile at *B*/8 position factor of safety against piping increases up to 22.00% compared to 3*B*/8 position whereas this is approximately

18.18% for 2*B*/8 position, compared to 3*B*/8 position. It is also observed that factor of safety against piping increases by 20–30% due to increase in sheet pile length.

5 Conclusions

The following conclusions may be drawn from this present study:

1. Effectiveness of seepage cut off has been appropriately studied in centrifuge modeling through image-based analysis.
2. Sheet pile length increases the seepage path, which reduces the exit gradient. In case of an increase of sheet pile length by 30% of the bottom width of the dam the exit gradient decreases 9.97%. Furthermore, when sheet pile length increases 59% of the bottom width of the dam, the exit gradient decreases 18.16%.
3. Exit gradient decreases by 8.17% if the sheet pile position is shifted from 14.25% of bottom width of the dam from the downstream end.
4. For any fixed position when sheet pile length increases seepage path increases. Fluid flow vector decreases as sheet pile moves toward downstream end and it is maximum for least length and flow vector reduces with the increase of sheet pile length studied through experimental modeling.
5. Fluid flow vector for 20 m length of sheet pile on the downstream end decreases 30% less compared to 5 m length of sheet pile and 13% less compared to 15 m length of sheet pile for any particular position of sheet pile.
6. Factor of safety against piping decreases 18% when sheet pile position moves away from downstream end for a fixed sheet pile length. As the length of the sheet pile increases the factor of safety against piping also increases. In the case of piping, it is more predominant due to the increase in creep length. The factor of safety against piping increases by 20–30% due to an increase of sheet pile length.

References

1. Foster, M., Fell, R., Spannagle, M.: The statistics of embankment dam failures and accidents. Canadian Geotech. J. **37**(10), 1000–1024 (2000)
2. McCook, D.: A Comprehensive discussion of piping and internal erosion failure mechanisms. In: Proceedings of the 2004 Annual Association of State Dam Safety Officials, 1–6 (2004)
3. Fell, R., Wan, C.F.: Methods for estimating the probability of failure of embankment dams by internal erosion and piping-piping through the foundation and from embankment to foundation. UNICIV Report No R-436, The University of New South Wales, Sydney, 2052, Australia. ISBN: 85841 403 1 (2005)
4. Aral, Mustafa M., Maslia, Morris L.: Unsteady seepage analysis of Wallace dam. J. Hydraul. Eng. **109**, 809–826 (1983)

5. Davies, M.C.R., Parry, R.H.G.: Centrifuge modelling of embankments on clay foundations. Soils Found. **25**(4), 19–36, December 1985, Japanese Society of Soil Mechanics and Foundation Engineering (1985)
6. Perri, J.F., Shewbridge, S.E., Cobos-Roam D.A., Green, R.K.: Steady state seepage pore water pressures influence in the slope stability analysis of levees. In: GeoCongress, ASCE (2012)